INTERNATIONAL JOURNAL OF NUMERICAL MODELLING: ELECTRONIC NETWORKS, DEVICES AND FIELDS
*Int. J. Numer. Model.* 2007; **20**:237–252
Published online 10 April 2007 in Wiley InterScience (www.interscience.wiley.com). DOI: 10.1002/jnm.645

# An investigation into time domain Doppler modelling using the TLM numerical method

I. J. G. Scott and D. de Cogan*,†

*School of Computing Sciences, University of East Anglia, Norwich NR4 7TJ, U.K.*

SUMMARY

The effects observed by a moving source and stationary receiver, or conversely stationary source and moving receiver are well known to physicists. The Doppler effect as it is commonly known is recognized as a perceived change in frequency of the incident signal upon the receiver, caused by the motion of either the source or receiver with respect to the stationary component, occurring in both electromagnetic (transverse) and acoustic (longitudinal) waves. This paper will primarily focus on the acoustic Doppler effect in the time domain, simulating a variety of scenarios using transmission line matrix (TLM) modelling in which the effect can be observed, proceeding to compare the accuracy of the various models generated. A new technique to allow arbitrary placement of boundaries of a TLM mesh will also be introduced and analysed allowing accurate placement of the moving walls within the simulation. Copyright © 2007 John Wiley & Sons, Ltd.

Received 1 July 2006; Accepted 30 January 2007

KEY WORDS: Doppler effect; transmission line matrix modelling; boundary conforming mesh; moving media; time-domain numerical modelling; numerical dispersion

## 1. INTRODUCTION

If we assume a model with moving source and stationary receiver, the observer positioned at the receiver will perceive an increase in frequency (decrease in wavelength) as the source is approaching and a decrease in frequency (increase in wavelength) as the source moves away. This can be most easily explained by looking at the waves emitted from a point source in the time domain. If we imagine the scenario illustrated by Figure 1 where $k$ represents the discrete time index, the source can be thought of as injecting a signal at each moment in time as it moves towards a stationary receiver. As can be seen the signal radiating from the source is effectively 'stacked' in the time domain, meaning for a stationary source the three injected values will be

*Correspondence to: D. de Cogan, School of Computing Sciences, University of East Anglia, Norwich NR4 7TJ, U.K.
†E-mail: ddc@cmp.uea.ac.uk

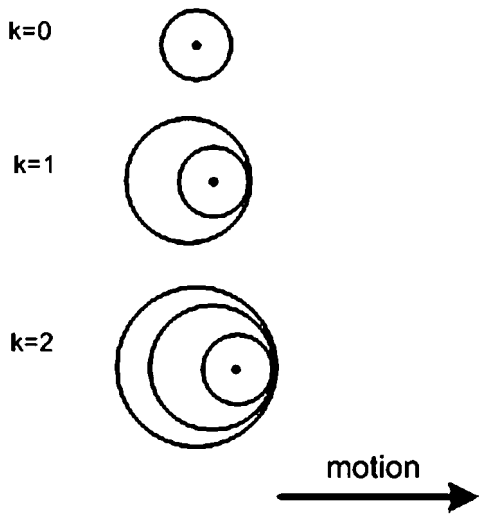


Figure 1. Illustration of acoustic emissions from a moving source.

received almost simultaneously, appearing to reduce the wavelength of the signal and hence increase the frequency. However, as can also be observed if a receiver is moving at the same speed as the source (in the same direction), the signals received will be delayed by the same amount as those transmitted are 'stacked' in time, meaning no difference in transmitted to received signal would be observed. In a similar manner, if the receiver was moving towards the source, the effect would become elaborated, causing a further increase in observed frequency.

All this is well known and used in a wide variety of modern applications, however, numerical modelling of the phenomena is rarely performed, relying on experimental confirmation and analytical models for most applications. Cabeceira *et al.* [1] discuss and implement a Doppler simulation using the transmission line matrix (TLM) numerical method. Their work focuses on moving the medium as apposed to the source or receiver; this is an equivalent formulation that transposes the problems observed by moving sources in TLM (as will be illustrated in Section 3) to the boundaries of the mesh, which will be studied in Section 4. An alternative TLM approach was proposed by O'Connor [2], this suggests keeping the medium stationary while moving the source, using a modified approach to account for dispersive effects at the source, this will be analysed further in Section 3.

This paper attempts to collate the work of previous authors to model the Doppler effect and then continues to propose a new method, improving slightly on the results in available literature. We will begin with an introduction to the TLM numerical method, indicating the procedure and formulation relevant to the current situation, a more formal and of greater depth introduction can be found in the relevant literature [3,4], this section will then continue to introduce two boundary conforming schemes, the first proposed by Mueller *et al.* [5], and the second, a new technique attempting to limit the drawbacks of the Mueller *et al.* approach, these will become useful in Section 4 where the TLM mesh will be moved to simulate the effect of a moving medium and hence boundary placement between nodes will be required. Before this is attempted some approaches to moving the source within a stationary mesh will be analysed in Section 3,



DOI: 10.1002/jnm

indicating the errors obtained which we attempt to circumvent in Section 4. Section 5 attempts to conclude the observations made throughout the experiments.

## 2. TRANSMISSION LINE MATRIX MODELLING

The numerical modelling method known as TLM was first proposed by Johns and Beurle [3] in 1971. The method proceeds by attempting to model physical scenarios using electrical analogues. A basic 2D scalar TLM node is illustrated in Figure 2 (with neighbouring nodes). The interconnections between nodes are representative of lossless transmission lines of finite length, with intrinsic impedance $Z_0$. The standard electromagnetic formula,

$$Z_{\text{obs}} = Z_0 \frac{Z_L + Z_0 \tanh(\beta \Delta x/2)}{Z_0 + Z_L \tanh(\beta \Delta x/2)} \tag{1}$$

where $\beta = 2\pi/\lambda$ and $\lambda$ is the wavelength, can be used to describe the observed impedance of a line of length $\Delta x/2$ with termination $Z_L$ and intrinsic impedance $Z_0$. As can be seen from Figure 2, for internal nodes $Z_L = Z_0$, causing the observed impedance to equal the intrinsic impedance.

When the terminating impedance does not match the intrinsic impedance of the line (as will be the case for the bounding walls of the TLM mesh), the proportion of reflected energy can be calculated using

$$\rho = \frac{Z_L - Z_0}{Z_L + Z_0} \tag{2}$$

the identifier $\rho$ is termed the reflection coefficient. As can be seen if the impedances match, $\rho = 0$ and hence all energy is transmitted into the connecting line. The energy transmitted is calculated as $\tau = (1 - \rho)/3$ for a 2D TLM node as illustrated by Figure 2. As can be seen from Figure 3, with an incident pulse on the west line, when the node is reached, the pulse will observe a terminating impedance of $Z_0/3$, i.e. it 'sees' the interconnecting north, south and east lines in parallel with respect to the west line. This gives a reflection coefficient ($\rho$) of $-\frac{1}{2}$ using Equation

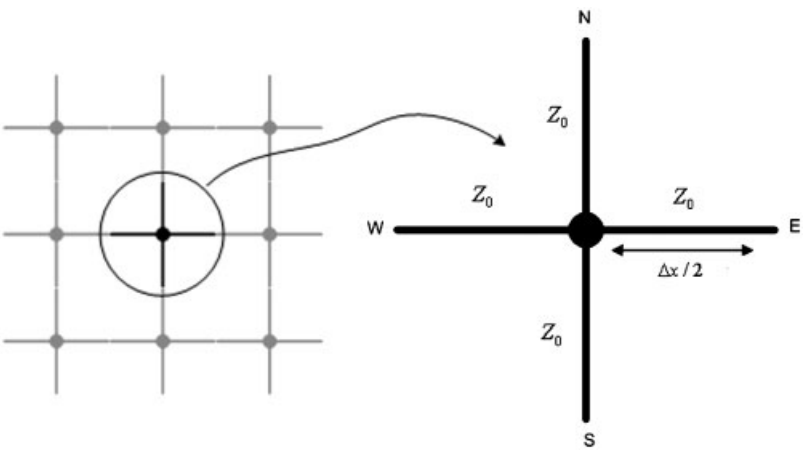


Figure 2. 2D TLM mesh and 2D scalar TLM node.



DOI: 10.1002/jnm

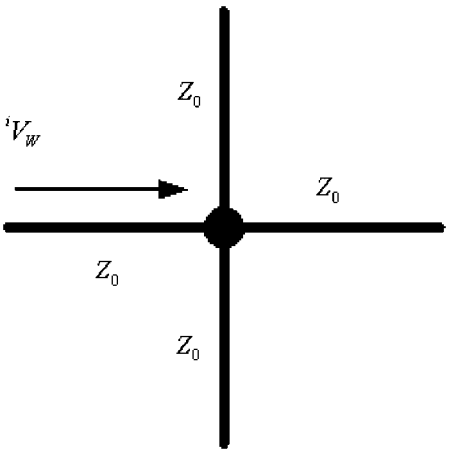


Figure 3. 2D TLM node illustrating incident pulse on West transmission line.

(2), and a transmission coefficient ($\tau$) of $\frac{1}{2}$ equally on the north, south and east lines. In the TLM iterative process this is usually termed as the scatter procedure, it is duplicated over the entire mesh of TLM nodes, this is most easily represented as a matrix equation of the form

$$\begin{pmatrix} {}^sV_{\mathrm{N}} \\ {}^sV_{\mathrm{S}} \\ {}^sV_{\mathrm{E}} \\ {}^sV_{\mathrm{W}} \end{pmatrix} = \frac{1}{2}\begin{bmatrix} -1 & 1 & 1 & 1 \\ 1 & -1 & 1 & 1 \\ 1 & 1 & -1 & 1 \\ 1 & 1 & 1 & -1 \end{bmatrix} \begin{pmatrix} {}^iV_{\mathrm{N}} \\ {}^iV_{\mathrm{S}} \\ {}^iV_{\mathrm{E}} \\ {}^iV_{\mathrm{W}} \end{pmatrix} \tag{3}$$

where ${}^iV_{\mathrm{N}}$ represents the incident voltage in the north direction, ${}^sV_{\mathrm{N}}$ represents the scattered voltage to the north, etc., these are effective matrices containing the values for each node within the mesh. These matrices can be indexed using a normal 2D co-ordinate system (i.e. origin in the bottom left), in this manner using $(x, y)$ for horizontal and vertical displacement, respectively, the incident stage of the TLM routine can be represented by

$$\begin{aligned} {}_{k+1}{}^iV_{\mathrm{N}}(x,y) &= {}_k{}^sV_{\mathrm{S}}(x,y+1) \\ {}_{k+1}{}^iV_{\mathrm{S}}(x,y) &= {}_k{}^sV_{\mathrm{N}}(x,y-1) \\ {}_{k+1}{}^iV_{\mathrm{E}}(x,y) &= {}_k{}^sV_{\mathrm{W}}(x+1,y) \\ {}_{k+1}{}^iV_{\mathrm{W}}(x,y) &= {}_k{}^sV_{\mathrm{E}}(x-1,y) \end{aligned} \tag{4}$$

i.e. the incident potential at node $x, y$ at discrete time step $k+1$ in the north direction is equivalent to the potential scattered from the south line of the node above at the previous time $k$. This process is repeated for all nodes inside the TLM mesh, identical to the scattering procedure. These procedures taken collectively form the basis of the TLM iterative procedure, and hence describe a method for propagating a signal within a discrete TLM simulation.



DOI: 10.1002/jnm

In order for the potential of a finite node within the 2D TLM mesh to be observed at any discrete time step $k$, it is necessary to take the sum of currents on adjacent lines and divide by the sum of admittances

$$ {}_k\phi(x,y) = \frac{\left[\frac{2^iV_N}{Z_0} + \frac{2^iV_S}{Z_0} + \frac{2^iV_E}{Z_0} + \frac{2^iV_W}{Z_0}\right]}{\left[\frac{1}{Z_0} + \frac{1}{Z_0} + \frac{1}{Z_0} + \frac{1}{Z_0}\right]} $$

Simplifying

$$ {}_k\phi(x,y) = \frac{[{}^iV_N + {}^iV_S + {}^iV_E + {}^iV_W]}{2} \tag{5} $$

This is found by forming the Thévenin equivalent network and solving for $\phi$ (the potential at the node point) [4]. Equation (5) can be used at any discrete multiple ($k$) of $\Delta t$ (time), to observe the potential existent on any node $(x, y)$. This completes our introduction to TLM, a more in depth review is given in [3,4].

### 2.1. Introduction to the BMH boundary conforming scheme

The boundaries of an acoustic scenario (pressure release or rigid) can be described in TLM by sufficient selection of the terminating impedance. For a pressure release boundary, $Z_L$ is set equal to 0, i.e. effectively short circuit conditions, this gives a reflection coefficient ($\rho$) of $-1$ from Equation (2). Likewise a similar argument is presented for a rigid boundary, interpreting $Z_L$ as an open circuit, i.e. $Z_L \to \infty$ and $\rho = 1$. These formulations are the basic starting point to describe the boundaries of the mesh, however, as can be identified from Figures 2 and 3, the lengths of transmission line from each node within the mesh are set at $\Delta x/2$, giving a distance to each boundary a discrete value. While this may be acceptable for uniform structures, curved boundaries, or arbitrary placed linear boundaries will not fall an exact multiple of $\Delta x/2$ from the bounding nodes, for example, in Figure 4, it can be seen the sloping boundary will cut the east section of transmission line between 0 and $\Delta x$. While some numerical modelling schemes (finite differences for example) [6] are able to adjust the lengths of interconnecting lines to meet with boundaries, due to the discretized nature of time within a TLM mesh, this is not possible.

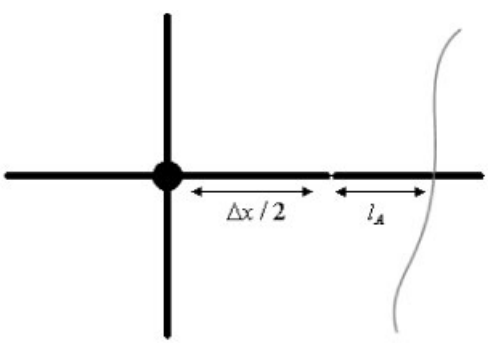


Figure 4. Arbitrary placed bounding wall after the $\Delta x/2$ line end.



DOI: 10.1002/jnm

For example, in Figure 4 a pulse scattered on the east line will reach the boundary at time $(k+1/2)\Delta t$ and arrive back, incident upon the node at time $(k+1)\Delta t$. If the length of the line was changed to match a boundary location exactly this may become less or greater than $(k+1)\Delta t$, losing the discrete time nature of the TLM procedure and will hence cause the TLM routine to become unstable. For this reason other approaches are required to more accurately describe a boundary, while maintaining the rules of the TLM procedure. One obvious approach is to increase the resolution of the TLM mesh, hence increasing the number of nodes and reducing $\Delta x$; however, this greatly increases the computational load of the algorithm so will not be considered further.

A popular technique proposed by Mueller *et al*. [5] suggests a recursive definition to describe arbitrary placed boundaries of the mesh. An imaginary reference plane is located a distance $\Delta x/2$ from the node. The arbitrary perfectly reflecting boundaries of the mesh are then described using

$$ {}_{k}V^{i} = \rho \frac{1-\kappa}{1+\kappa} k^{V^{r}} + \frac{\kappa}{1+\kappa}(\rho_{k-1}V^{r} +_{k-1} V^{i}) \tag{6} $$

where ${}_{k-1}V^{i}$ and ${}_{k-1}V^{r}$ represent the incident and reflected (scattered) pulses at time $k-1$, respectively. The reflection coefficient $\rho$ is identical to that described by Equation (2). $\kappa = \sqrt{2l_A/\Delta x}$, where $l_A$ is the true distance to the boundary after the $\Delta x/2$ line end (as illustrated in Figure 4). As can be seen if the boundary 'cuts' before the placement of the reference plane at $\Delta x/2$, Equation (6) cannot be used. In this case the node is removed and the neighbouring node taken to be the boundary adjacent one. In this case $l_A$ becomes $l_A + \Delta x$, the exclusion of the node causes an extra error to be included in the simulation which was not evident in the stepwise approach, however, this appears to make little difference.

While this technique is well founded and increases the accuracy of a TLM simulation substantially [7], the extra memory and time required, either to store previous results for the recursion, or to regenerate previous values, can prove almost as limiting as increasing the mesh resolution, for these reasons we propose an alternative approach in the following section, attempting to limit these 'shortfalls.' For the remainder of this paper the approach just analysed will be termed as *BMH*.

### 2.2. *Improved boundary conforming scheme*

As mentioned the main drawback of the BMH method is the recursion caused by the placement of the reference plane. However if the reference is taken at the node, the need for recursion is removed and a much simpler formulation can be generated. This section details a new scheme adhering to this observation. We propose performing an impedance transformation on the sections of transmission line connecting with the boundary, to accurately describe the location of the boundary, while allowing the time and discrete nature of the TLM mesh to remain intact.

The observed impedance of a line of length $l_A$ with intrinsic impedance $Z_0$ and terminating impedance $Z_L$ (Figure 5) can be found from Equation (1) as

$$ Z_{\text{obs}} = Z_0 \frac{Z_L + Z_0 \tanh(\beta l_A)}{Z_0 + Z_L \tanh(\beta l_A)} \tag{7} $$



DOI: 10.1002/jnm

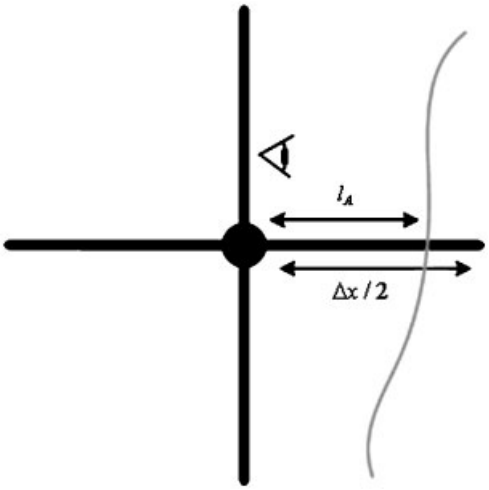


Figure 5. Illustration of scenario for impedance transformation, observer placed at node.

where the observer is at the node. Using the low-frequency approximation underlying TLM, the intrinsic impedance $Z_0$ of the line can be expressed in terms of the capacitance per unit length as well as the spatial and temporal discretizations of the model

$$Z_0 = \frac{\Delta t/2}{C_d \Delta x/2} = \frac{\Delta t'}{C_d l_A} \tag{8}$$

This suggests we can replace the line of length $l_A$ with an equivalent line of length $\Delta x/2$ adjusting the impedance to counter act the difference in length, allowing the signal to arrive back at the node at time $(k+1)\Delta t$ while appearing to have travelled to the true boundary location.

For the case when $\rho = 1$ (i.e. rigid boundary), Equation (7) can be simplified to give

$$Z_{\text{obs}} = \frac{Z_0}{\tanh(\beta l_A)} \tag{9}$$

However, for an equivalent transmission line of length $\Delta x/2$, we obtain

$$Z_{\text{obs}} = \frac{Z_A}{\tanh(\beta \Delta x/2)} \tag{10}$$

where the intrinsic impedance of the line has been adjusted to account for the change in length. Assuming a low-frequency model, the hyperbolic tangent can be approximated by its argument, therefore (9) and (10) become, respectively,

$$Z_{\text{obs}} = \frac{Z_0}{\beta l_A} \quad \text{and} \quad Z_{\text{obs}} = \frac{Z_A}{\beta \Delta x/2} \tag{11}$$

Since a pulse at the node should see an identical impedance whether the line is of length $l_A$ or $\Delta x/2$, these equations can be equated, giving

$$\frac{Z_0}{\beta l_A} = \frac{Z_A}{\beta \Delta x/2} \tag{12a}$$



DOI: 10.1002/jnm

rearranging

$$Z_A = Z_0 \left[\frac{\Delta x}{2l_A}\right] \tag{12b}$$

Using a similar analysis for a pressure release boundary, i.e. $Z_L \to 0$ giving $\rho = -1$, we obtain equivalent formulations of Equations (9) and (10)

$$Z_{\text{obs}} = Z_0 \tanh(\beta l_A) \quad \text{and} \quad Z_{\text{obs}} = Z_A \tanh(\beta \Delta x/2) \tag{13}$$

Proceeding as before and assuming low frequencies we obtain after simplification

$$Z_A = Z_0 \left[\frac{2l_A}{\Delta x}\right] \tag{14}$$

Equations (12b) and (14) can then be used to describe arbitrary placed boundaries that fall between discrete multiples of the models discretization $\Delta x$. Unlike the BMH (Beyer, Mueller, Hoefer) model, the approach taken here allows $l_A$ to be between 0 and $\Delta x$, meaning node removal is no longer required. The recursive nature increasing time and space requirements of the BMH approach is also removed, however, Equation (5) in simplified form can no longer be used, as the intrinsic impedance for boundary adjacent sections of transmission line can no longer be assumed equal. This approach will be termed *uniform* in the remainder of this paper.

## 3. MOVING SOURCE STATIONARY OBSERVER

To formulate a Doppler model for a moving source, it is necessary to place the boundaries of the computation space a significant distance from the source to prevent interference from reflected signals. While it is possible to define a perfectly matched layer (PML) to allow the signal moving off a TLM mesh to be absorbed, for this scenario it is not necessary as the mesh can easily be enlarged and still remains within acceptable computational limits, this also prevents any extra errors from being introduced into the model.

To move a sinusoidal point source within a discrete TLM mesh, to allow the source to land on nodes, it is necessary to move in integer multiples of $\Delta x$. However, if this is performed, moving one node on each time step $\Delta t$ is the equivalent of mach 1 within the mesh, producing interesting although unpractical results [8]. For this reason it is necessary to move between nodes, standard TLM however, as described in Section 2 does not provide this mechanism, therefore to move at a velocity of 0.2 within the mesh is effectively the equivalent of traversing one node every 5 iterations (discrete time steps of the algorithm). If this is performed in a TLM mesh of size 601 by 601, with $\Delta x$ set to 1, placing a sinusoidal point source of wavelength 20 nodes at node 270 across and centred in the vertical direction, the results of Figure 6 are generated. This has been run for 270 iterations, allowing the source to move in the positive (east) horizontal direction. As can clearly be seen, dispersive effects created by the motion of the source are generated, producing bow and stern waves about the source. We can perform a Fourier transform on locations about the source, to verify the shift in frequency we would expect from a Doppler model. The results using a Fourier transform sampling at 10 kHz are as shown in Figure 7. As can be seen, the shift in frequency behind and in front of the source is as expected, however, there are also large spurious harmonics present behind the source, generated by the distortion



DOI: 10.1002/jnm

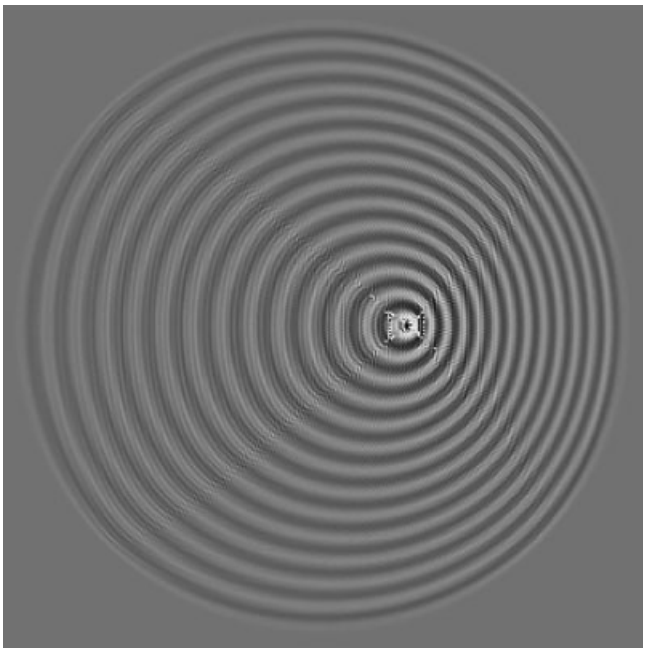

Figure 6. Sinusoidal point source, moving in the horizontal direction (east) 601 by 601 mesh resolution, source moves 1 node every 5 iterations.

from the movement in the source. This, however, is as expected due to the discrete nature of the motion.

An explanation for the spurious harmonics is proposed in [4]. The phenomenon of numerical dispersion, whereby the velocity relies on frequency and direction helps to describe the dispersion seen around a stationary point source. The signal along the diagonals in a rectangular mesh will appear to travel at a slower velocity than that on the main horizontal and vertical. This velocity is in fact derived as $1/\sqrt{2}$ of the free-space velocity, this is found by observing how a signal will travel from one corner of an individual square of nodes within the mesh to another corner on the same diagonal, the distance $\sqrt{2}\Delta x$ will be traversed in time $2\Delta t$, giving a velocity of $(1/\sqrt{2})\Delta x/\Delta t$. This fluctuation in velocity, dependant on the direction of the signal, causes the signal within the mesh to contain small dispersive effects, these appear to become elaborated when the source is moving. For a stationary sinusoidal point source, the dispersive effects are insignificant providing $\Delta x/\lambda < 0.1$ [4]. For a single shot pulse this is not the case, as a collection of all frequencies supported by the TLM mesh will be contained at the source. For a moving sinusoidal point source, the 'inject-and-forget' behaviour of the source effectively creates a single shot pulse at each individual location, meaning some frequencies where $\Delta x/\lambda > 0.1$ will exist causing a kind of dispersive effect like that seen about a stationary single-shot point source. However, as the source is moving in this simulation, the dispersive effects seen along the diagonals for a stationary single-shot point source will also move, effectively forming along a separate diagonal dependant on the position of the source at each iteration, it is this effect that generates the bow and stern waves seen about the source in Figure 6.



DOI: 10.1002/jnm

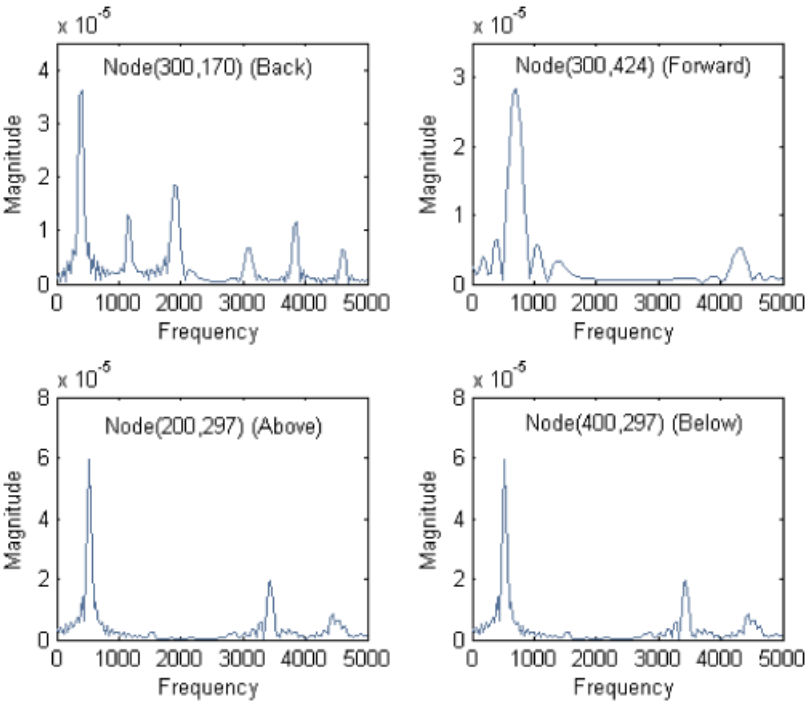


Figure 7. Fourier transform about moving source implementing stepped scheme, illustrating frequencies observed at stationary locations, node locations are given as $(y, x)$ with origin at top left.

In Figure 8 this can be seen more clearly. For a source beginning at discrete time $k = 0$, the dispersion is as usual, however, at $k = 1$ the next value will be injected to the right of the previous value, at this same time the first injected pulse will begin to disperse, meaning the second value is offset in both space and time from the first. As can be identified from the figure, the offset in space will cause the dispersive effects seen along the diagonals to appear along bow and stern waves at angles dependant on the speed of the moving source. Analysis of this is performed in [4], arriving at two formulae to calculate the angle between the forward and aft waves dependant on the speed of the source. However, this may also provide a more rigorous explanation as to why the dispersive effects present themselves here, while remaining insignificant for a stationary sinusoidal source. As can be seen from Figure 8, if the pulses are offset in time as well as space, the value injected at time $k = 0$ will have a value of $+$ve at time $k = 0$. At time $k = 1$, the new injected value will have a value of $+$ve at the current source location, while the previous injected value will have dispersed to that location and also be $+$ve, however, if the source is stationary, the new injected value will still be $+$ve, but the old injected value will now be $-$ve (as the source will still be at the original node), in this manner the new injected value will cancel some of the old value, however, when the source is moving this is not performed. This may help to explain the dispersive effects observed in moving source simulations using differential space time modelling techniques.



DOI: 10.1002/jnm

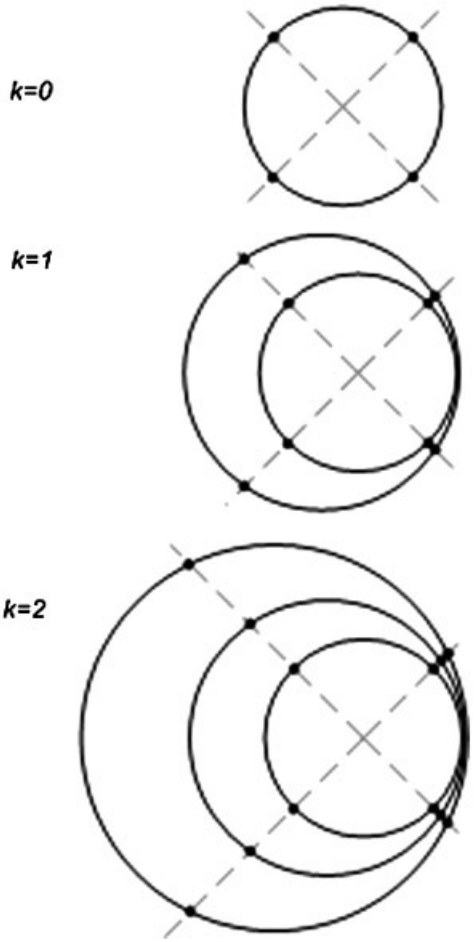


Figure 8. Illustration of moving sinusoidal point source within a rectilinear TLM mesh.

O'Connor [2] proposes a method which injects a percentage of the source energy at neighbouring nodes, dependant on how close the source is to each node. For example in 1D if the node begins at node $(x, y)$ 100% of the energy is injected at that node, if at time $(k+1)\Delta t$, the source is at position $(x+\Delta x/4, y)$, one quarter of the energy will be injected at node $(x+1, y)$, leaving three quarters for node $(x, y)$, etc. As can be seen from Figure 9, this approach seems to improve results for Fourier transforms taken in front, above and below the source, however, it appears to increase the fluctuations in the frequency domain seen behind the source.

If we attempt to perform an impedance transformation as per Section 2.2 [9] the results (Figure 10) are improved slightly, reducing some of the dispersive effects seen behind the source further than in the stepped and O'Connor solutions. However, they appear to be unable to cancel the erroneous harmonics in front, above and below the source which the O'Connor method managed fairly well.



DOI: 10.1002/jnm

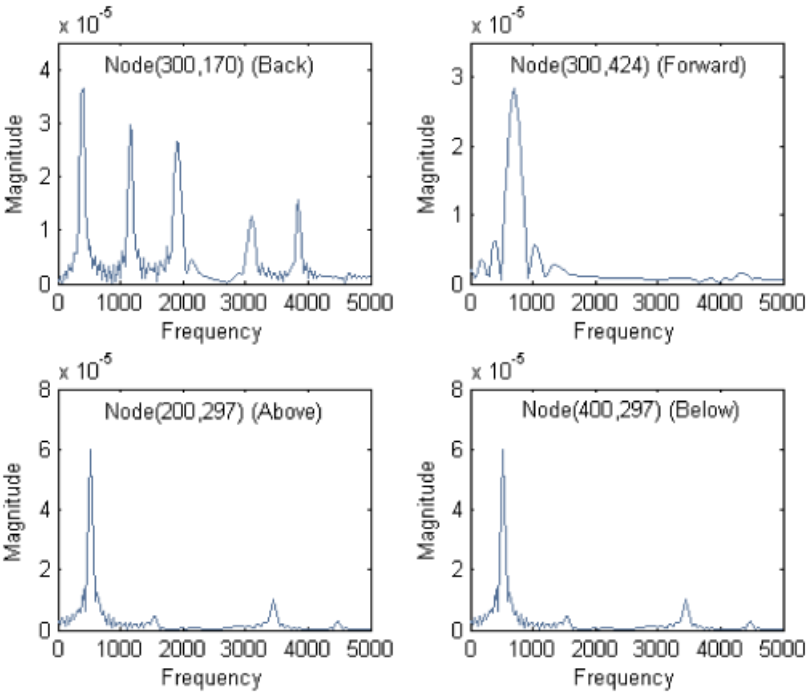


Figure 9. Fourier transform about moving source implementing O'Connor placement method, illustrating frequencies observed at stationary locations, node locations are given as $(y, x)$ with origin at top left.

In light of these findings it may prove productive to move the medium (mesh) rather than the source, this transposes the problem to the boundary of the computation space, however, we are now able to fully utilize the boundary conforming schemes described in Sections 2.1 and 2.2.

## 4. MOVING MEDIUM STATIONARY OBSERVER

To duplicate the effect of a moving medium, it is necessary to move the entire TLM computational space upon each iteration, this is equivalent to moving the boundaries of the mesh. Again, as in the case of the moving source the boundary should not be moved in integer multiples of nodes, as the velocity would become to great to allow the Doppler effect to be observed, this is why the boundary conforming schemes are useful, allowing accurate placement between nodes.

If we move the medium at a rate of 1 node every 5 iterations, using a stepwise scheme, i.e. closest node approximation, in the negative $x$ direction, with a sinusoidal point source at node (1991,181) (total mesh size is 2401 by 361 nodes) with frequency 500 Hz and east and west boundaries of $\rho = 1$ (i.e. rigid boundary in acoustics), the plot of Figure 11 is obtained. Note the north and south boundaries are defined as PMLs, a more in-depth discussion of this topic is provided in [10]. The formal operation of a PML is to allow the signal moving towards the



DOI: 10.1002/jnm

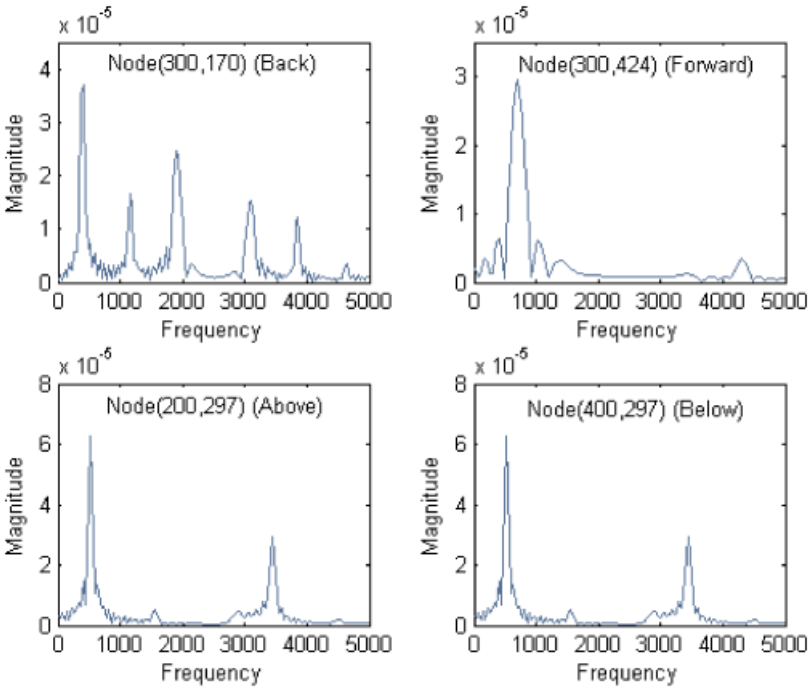


Figure 10. Fourier transform about moving source implementing impedance transformation scheme, illustrating frequencies observed at stationary locations, node locations are given as $(y, x)$ with origin at top left.

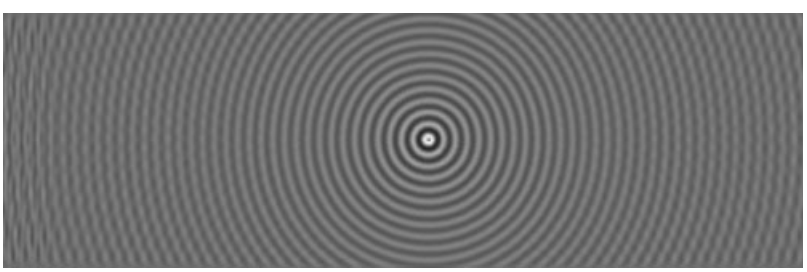

Figure 11. Doppler effect observed in TLM simulation, with moving medium (mesh), implementing stepped TLM scheme. Surface view generated using Equation (5).

so-defined boundary, to be absorbed and hence no reflection is observed, this was not necessary in the moving source simulations, however, space limitations here require their use. The simulation is then run for a total of 2048 iterations, allowing a fast fourier transform to be performed at the east and west boundaries (centred in the $y$-axis). The results are shown in Figure 12 compared against an identical simulation with a stationary medium. As can be seen, there is the expected shift in frequency behind and in front of the source however there are also some relatively large



DOI: 10.1002/jnm

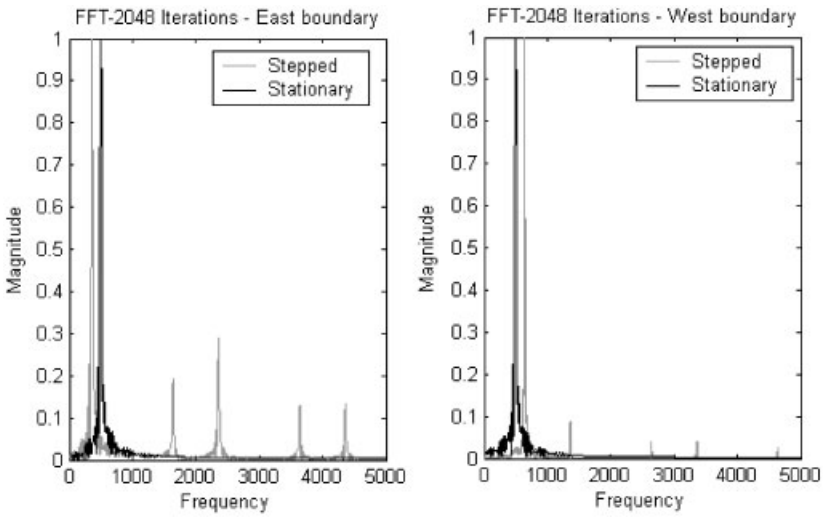


Figure 12. Fourier transform performed at the west and east boundaries of TLM Doppler simulation, implementing stepped boundary placement scheme.

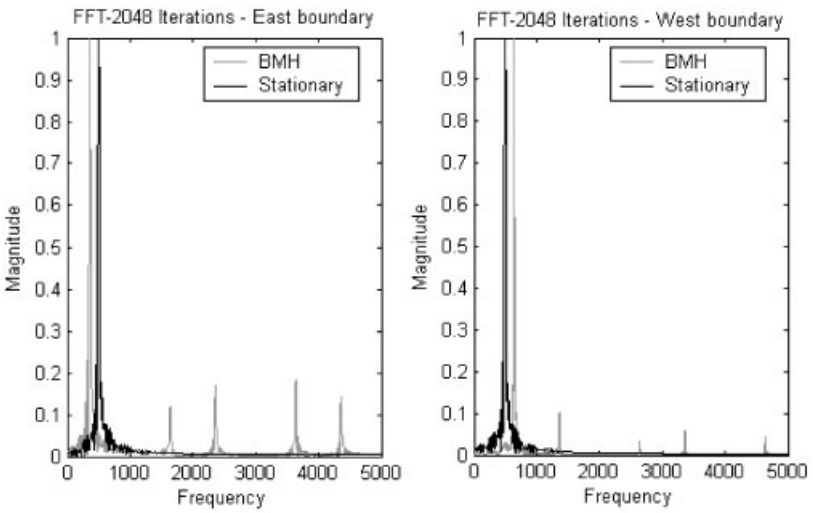


Figure 13. Fourier transform performed at the west and east boundaries of TLM Doppler simulation, implementing BMH boundary placement scheme.

multiples of the fundamental frequency present. If we define the distance between the shifted primary harmonic and stationary primary harmonic as $\Delta f$, the amount by which the harmonics measured in front and behind the source will differ from one another is $2\Delta f$.

If we perform the same analysis using the BMH technique outlined in Section 2.1, the results of Figure 13 are obtained. As can be seen and would be expected, these are a slight improvement on the stepped scheme, reducing the multiples of the primary harmonic in the Fourier



DOI: 10.1002/jnm

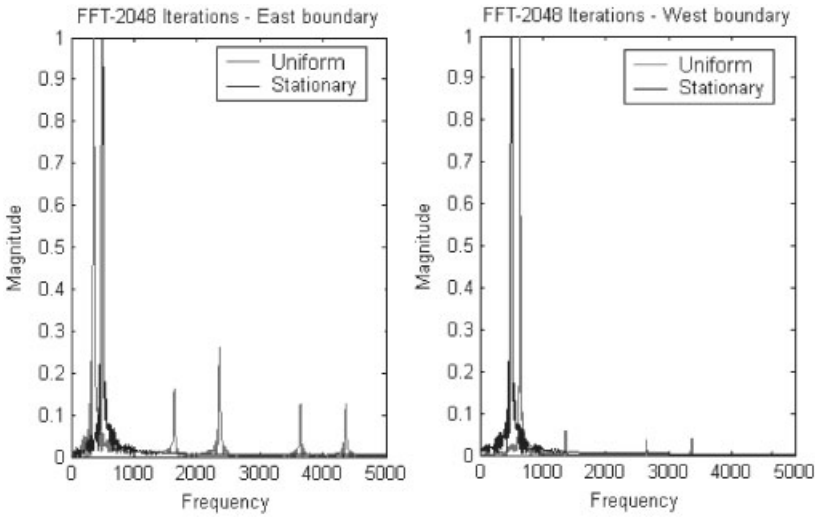


Figure 14. Fourier transform performed at the west and east boundaries of TLM Doppler simulation, implementing impedance transformation of Section 2.2.

transforms taken on the East boundary (behind the source). However, we now note a slight increase in errors on the West boundary. Due to the increase in time and memory caused by the recursive nature of the BMH approach this technique is not as appealing as that described in Section 2.2, if we perform an identical analysis using the uniform approach of 2.2, the results produced are shown in Figure 14. As can be seen, the harmonics of the primary on the East boundary appear to have increased slightly, as per the stepped version; however, there is now a considerable improvement against both the stepped and BMH approach for the west boundary. This increase in accuracy, unlike that for the BMH approach, is obtained with no extra computational burden.

## 5. CONCLUSIONS

In this paper we propose a novel technique to allow arbitrary placement of boundaries for the TLM numerical method, while attempting to limit the drawbacks of existing techniques. Due to the simplicity of the impedance transformations, the technique can be equally used by engineers with minimal mathematical knowledge, obtaining a wider audience than some of the more complicated boundary conforming schemes proposed in recent years.

Doppler modelling using simple TLM has displayed the expected frequency shifts, but in addition there are harmonics that appear unphysical. Our investigations have shown that these still persist even when more sophisticated TLM schemes are used.

A comparison of the impedance transformation approach proposed in Section 2.2 has been performed for moving arbitrary placed boundaries, against traditional approaches (BMH and stepwise), noting the significant increase in accuracy against the stepped approach and results in tier with those produced by the BMH approach, with no additional computational overhead.



DOI: 10.1002/jnm

A brief explanation is provided to describe the effects seen about a moving source by comparing with an identical analysis for a stationary single-shot point source, the dispersive effects also exhibit for a moving boundary. It appears these are a factor of differential methods of space time modelling and as such cannot be completely removed, however, dependant on the model used, their effects can be considerably reduced.

## REFERENCES

1. Cabeceira ACL, Barba I, Grande A, Represa J. TLM simulation of electromagnetic wave propagation in anisotropic moving media. *International Journal of Numerical Modelling*: *Electronic Networks*, *Devices and Fields* 2005; **18**: 227–236.
2. O'Connor WJ. TLM model of waves in moving media. *International Journal of Numerical Modelling*: *Electronic Networks*, *Devices and Fields* 2002; **15**:205–214.
3. Johns PB, Beurle RL. Numerical solution of 2-dimensional scattering problems using a transmission line matrix. *Proceedings of the IEE* 1971; **118**:1203–1208.
4. de Cogan D, O'Connor WJ, Pulko S. *Transmission Line Matrix Modelling in Computational Mechanics*. Taylor & Francis, CRC Press: London, 2006.
5. Mueller U, Beyer A, Hoefer WJR. Moving boundaries in 2-D and 3-D TLM simulations realized by recursive formulas. *IEEE Transactions on Microwave Theory and Techniques* 1992; **40**(12):2267–2271.
6. Kreyszig E. *Advanced Engineering Mathematics*. Wiley: Chichester, 1999; 971–976.
7. Scott IJG, de Cogan D. Improved mesh conforming boundaries for the TLM numerical method. *PIERS* (*Progress in Electromagnetics Research Symposium*), Cambridge, MA, March 2006; 336–343.
8. Jaycocks R, Pomeroy SC. The precise placement of boundaries within a TLM mesh with applications. *TLM*: *the Wider Applications*. Proceedings of an informal meeting held at the University of East Anglia, Norwich (27 June 1996), School of Computing Sciences (UEA), Norwich, 1996 (ISBN 1 898290 01 6); 2.1–2.5.
9. de Cogan D, Hindmarsh D, Flint J. Doppler modelling and boundary conforming meshes. *First International Workshop on Generalised Applications of TLM and Related Techniques*, Czestochowa, June 2004.
10. Peña N, Ney MM. Absorbing-boundary conditions using perfectly-matched-layer (PML) technique for three-dimensional TLM simulations. *IEEE Transactions on Microwave Theory and Techniques* 1997; **45**:1749–1755.

## AUTHORS' BIOGRAPHIES

**Ian Scott** has studied at the School of Computing Sciences at the University of East Anglia for the degree of Computing Science with Electronics (BSc). His research interests include numerical methods for electromagnetic and acoustic simulations. He is currently a postgraduate research student at the University of Nottingham, U.K., investigating the use of time-reversal techniques in the TLM numerical method.

**Donard de Cogan** has a first degree in physical chemistry and a PhD in solid state physics from Trinity College, Dublin. He was on the teaching staff in electrical and electronic engineering at Nottingham University from 1978 to 1988. His initial research was concerned with the overload impulse withstand capability of a range of electrical and electronic components and the results confirmed a requirement for the numerical simulation of non-linear thermal processes. He was encouraged by Peter Johns to use the Transmission Line Matrix technique and as a result of inspirational guidance this soon became his principle line of research. In 1989 he transferred to the University of East Anglia at Norwich where he was promoted to Reader in 1994. He seeks to promote TLM to a wider audience and has recently co-authored *Transmission Line Matrix in Computational Mechanics* with Susan Pulko and William O'Connor. In July 2006 he retired from UEA and is now in Shanghai where he enjoys teaching engineering subjects to Chinese students who are planning a university career in the U.K.



DOI: 10.1002/jnm